Nanostructured Cu_2ZnSnS_4 thin films: influence of substrate temperature on structural, morphological, optical and electrical properties

M. Adelifard[1]

Abstract Photovoltaic Cu_2ZnSnS_4 (CZTS) thin films have been deposited on the glass substrate by a simple and low-cost spray pyrolysis technique without sulfurization treatment in a toxic atmosphere. The influence of the substrate temperatures on the structural, compositional, morphological, optical and electrical properties of the CZTS films was investigated. The formation of kesterite structure in the films was confirmed using X-ray diffraction measurements. The improved crystallinity of the CZTS with a (112) orientation was observed with increasing the substrate temperature. The band gap of all films was found to be in the range from 1.44 to 1.56 eV which is close to the ideal band gap for the highest theoretical conversion efficiency of solar cell. AFM analysis revealed a smooth, compact and crack-free morphology. The electrical studies showed that all these samples had a p-type conductivity, and the free hole density and mobility increased with increasing the substrate temperature.

1 Introduction

The quaternary Cu_2–II–IV–VI_4 compounds are considered to be a novel material for alternative thin-film solar cells (TFSC) owing to their p-type material with band gap energies from 0.96 to 1.63 eV [1]. Among these, Cu_2ZnSnS_4 (CZTS) is one of the most interesting materials, unlike other well-studied solar absorber materials such as Cu (In, Ga)(S,Se)$_2$ and CdTe, and contains only abundant and non-toxic elements. It could, therefore, bring much-needed cost reduction for thin-film solar cells. The CZTS exhibits an excellent optical absorption coefficient over 10^4 cm^{-1} and direct band gap energy of 1.4–1.6 eV, which makes this material especially suited for single-junction solar cells [2, 3].

Ito et al. [4] reported a CZTS thin-film solar cell for first time in 1988. They deposited CZTS thin films by atomic beam sputtering. Katagiri et al. [5–8] reported several studies on CZTS solar cells. The CZTS absorber layers in these studies were deposited by RF co-sputtering followed by vapor-phase sulfurization. All of these CZTS thin-film deposition processes were performed in a vacuum, and therefore, CZTS thin films produced were quite expensive, and it was also difficult to produce films with large areas. A chemical spray pyrolysis (CSP) technique is low-cost, non-vacuum and eco-friendly, and can be used for cost-effective large-area deposition, with no need of any sophisticated instrumentation. The composition, morphology, structural, electrical and optical properties of CZTS thin films, deposited by spray pyrolysis, can be tailored by changing the composition of precursors' solution and deposition parameters, especially the substrate temperature. According to our knowledge, only a few groups have studied spray deposition of CZTS thin films. Nakayama and Ito reported spray-deposited CZTS thin films followed by annealing the films under 5 % H_2S gas flow [9]. Kumar et al. [10, 11] studied the effects of substrate temperature, starting solution pH, copper salt and thiourea concentrations on the growth and properties of spray-deposited CZTS films. Structural, morphological and compositional characterization of as-deposited and annealed sprayed CZTS films was carried out by Kameyama et al. [12]. Espindola-Rodriguez et al. [13] used $CuCl_2$, zinc acetate dehydrate, $SnCl_4$ hydrate and thiourea as starting materials for the SPD coating solution. The precursor was annealed

✉ M. Adelifard
adelifard@du.ac.ir

1 School of Physics, Damghan University, Damghan, Iran

in S and Sn-containing atmosphere to obtain CZTS thin films. Shinde et al. [14] reported the thickness-dependent (244–754 nm) structural, morphological, optical and electrical properties of CZTS films. The effect of chlorine and carbon on sprayed CZTS thin-film solar cell was studied by Tanaka et al. [15].

In the present study, we have investigated the influence of substrate temperature on the growth and properties of CZTS thin films. We have achieved to this goal using an aqueous solutions of copper chloride, tin chloride, zinc chloride and thiourea at substrate temperatures of 260, 285, 310 and 335 °C without sulfurization in toxic atmosphere such as H_2S or 'S' vapor. Through this study, we have investigated the corresponding samples from various viewpoints, including: structural (crystallinity and surface morphology), optical (band gap energy estimation) and electrical (resistivity and Hall effect measurements) properties.

2 Experimental details

Cu_2ZnSnS_4 thin films were deposited on a 70×25 (mm)^2 glass substrate by spraying an aqueous solution containing a mixture of 0.1 M (0.8524 g) of $CuCl_2 \cdot 2H_2O$, 0.05 M (0.4307 g) of $ZnCl_2 \cdot 2H_2O$ and 0.05 M (0.8764 g) of tin chloride ($SnCl_4 \cdot 5H_2O$) in 50 ml double-distilled water. To enhance the solubility of tin chloride, a few drops of hydrochloric acid was also added to the solution. Then 0.4 M (1.5222 g) of thiourea ($CS(NH_2)_2$) was dissolved into the mixture. The excess quantity of thiourea was added to prevent any deficiency of sulfur in the prepared films because sulfur is a very volatile element, especially at elevated temperatures. The final solution was stirred for 30 min. Our previous studies for chalcogenide compound semiconductors, such as CuS thin films, have shown that sulfur source is volatile at higher temperature than 360 °C, which leads to the oxidation of copper sulfide. Also, on the basis of the obtained results for this compound [16], the optimized substrate temperatures for solar control coating applications was 285 °C. In this work, In order to investigate the effects of the substrate temperature on the composition, morphology, electrical and optical properties of sprayed Cu_2ZnSnS_4 thin films for solar cell applications, and also try to avoid any oxidation in the film growth, the substrate temperature of the studied samples was set at 260, 285, 310 and 335 °C with an accuracy of ±5 °C using a digital temperature controller. The samples are denoted as 'PV260,' 'PV285,' 'PV310' and 'PV335.' Other deposition parameters such as spray solution volume, spray deposition rate, nozzle-to-substrate distance and hot-plate rotation speed were maintained at: 50 ml, 5 ml/min, 30 cm and 50 rpm, respectively.

The crystalline structure was analyzed by X-ray diffraction (XRD) spectrum using a D8 Advance Bruker system using Cu–K$_\alpha$ radiation ($\lambda = 1.5406$ Å), and the optical characterization of the samples was performed by Shimadzu-UV1800 spectrophotometer in the spectral range of 400–1100 nm.

The roughness of the CZTS films was determined using Atomic Force Microscope model DME-95-50-E. The elemental composition was determined using an energy-dispersive spectrometer (EDS) system attached to VEGA2 SEM. Finally, the electrical resistivity and Hall effect data (magnetic field strength = 240 mT) of the samples were measured in the Van der Pauw configuration.

3 Results and discussion

3.1 Structural study

The structural analysis of CZTS thin films as a function of growth temperature was carried out by an X-ray diffractometer in 2θ range of 10°–70° as shown in Fig. 1. The broad hump in the range 2θ = 15°–35° is due to the amorphous glass substrate. The major peaks were identified comparing with JCPDS data file (card No: 026-0575) for Cu_2ZnSnS_4 corresponding to the (112), (220) and (116)
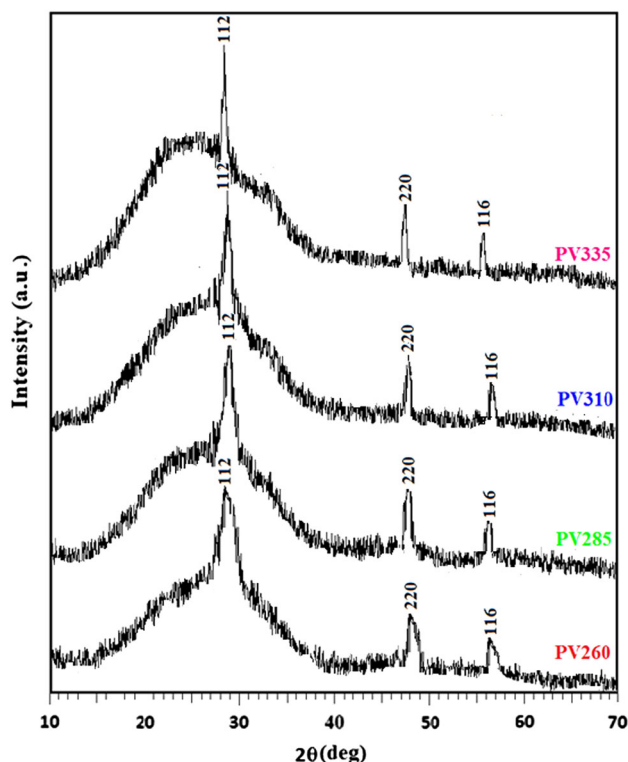

Fig. 1 XRD patterns of CZTS thin films deposited at various substrate temperature

reflections of kesterite (tetragonal system) structure. The CZTS thin films exhibit a major single diffraction peak (112), indicating a strongly preferred orientation in the (112) plane. The full width at half maximum (FWHM) of (112) peak of films becomes narrower as the substrate temperature goes up, indicating that high substrate temperature is helpful to crystallize.

Using Scherer's formula:

$$D = \frac{k\lambda}{\beta \cos\theta} \tag{1}$$

where D is the crystallite size, λ is the wavelength of the x-ray source, β is full width at half maximum of the main peak, k is a constant (close to unity) and θ is the Bragg angle, we found an estimation of the average crystallite size (D) in the studied samples, Table 1. The calculated crystallite sizes are found to be 6.98, 8.41, 11.94 and 18.89 nm for PV260, PV285, PV310 and PV335, respectively. The variation of the crystallite size has major influence on electrical properties of the samples, as described in the following.

3.2 Morphological study

To establish the role of substrate temperature, further study using atomic force microscopy was done. The AFM images are shown in Fig. 2. The AFM images show that the surfaces of the studied samples are rough and uniformly covered with spherical shaped grains. The grain size is <0.1 μm. However, these small grains seem to agglomerate to form larger grains. As seen in previous section, as the substrate temperature increases, the sharpness and intensity of (112) diffraction peak increases. Further, the value of roughness decreases from 35.6 to 21.4 nm (Table 1). Thus, the AFM study is consistent with XRD analysis of the studies samples.

3.3 Chemical composition dependence of Cu$_2$ZnSnS$_4$ thin films

Table 2 shows chemical compositions of Cu$_2$ZnSnS$_4$ thin films prepared in various substrate temperatures. The chemical composition ratio of Cu/(Zn + Sn) of the PV285 and PV310 thin films is larger than that of the precursor thin films, which illustrates that the elements of

Table 1 Crystallite size and roughness values of sprayed Cu$_2$ZnSnS$_4$ thin films

Film	PV260	PV285	PV310	PV335
Crystallite size (nm)	6.98	8.41	11.94	18.89
Roughness (nm)	35.6	33.3	29.2	21.4

Zn and Sn in the films are lost partly during the growth and that the lost amount of Sn is more than that of Zn in the CZTS films. From the Table 2, the CZTS thin films can be classified into two groups: S-poor state (i.e., S/metal <1, for the samples PV310 and PV335) and S content near the stoichiometry (for the samples PV260 and PV285), suggesting that the percentage of S is nearly dependent of the substrate temperature condition. Therefore, the percentage of S content in sprayed CZTS thin films can be approximately controlled by varying the substrate temperature.

3.4 Thickness measurement

The film thickness was measured using a Taly step profilometer (roughness detector with a stylus—Taylor Hobson model). Taly profile (a dedicated software package designed for use with laboratory instruments) has complete laboratory analysis functions such as: roughness parameters and step height measurement, etc., and the information can be displayed graphically and numerically. By step height measurement between coated glass and uncoated part of glass, we could determine the thickness of the studied samples with a precision of about 10 nm. The variation of film thickness against the substrate temperature is shown in Fig. 3. Inset of this figure shows the photographs of PV samples with different thicknesses obtained by varying the substrate temperature. As the substrate temperature increased, the film thickness first increased from 310 nm in PV260 sample to a maximum of 330 nm in PV285 sample and then decreased to about 270 nm. For higher substrate temperatures, the decrease in film thickness could be due to the loss of sulfur during pyrolysis (see Table 2).

3.5 Optical study

Optical transmission spectra in the range of 400–1100 nm for as-deposited PV samples are shown in Fig. 4. In the shorter wavelength region, the transmission of all samples increases with wavelength, while it raised sharply to about 24 % in the near-infrared (NIR) region with the exception of PV285 sample, whose peak transmittance has occurred around 17 %. Transmission is mainly depending on the composition and thickness of the films. A comparison between samples with different substrate temperatures shows that the sulfur-poor samples (PV310 and PV335 samples) have a higher transmittance than those with higher sulfur concentrations (PV310 and PV335 samples). This could be due to their higher conductivity, as discussed in Sect. 3.6. Also, according to the results of measurements for the thickness of the studied samples (Fig. 3), lower transmittance of PV285 sample in NIR region as compared
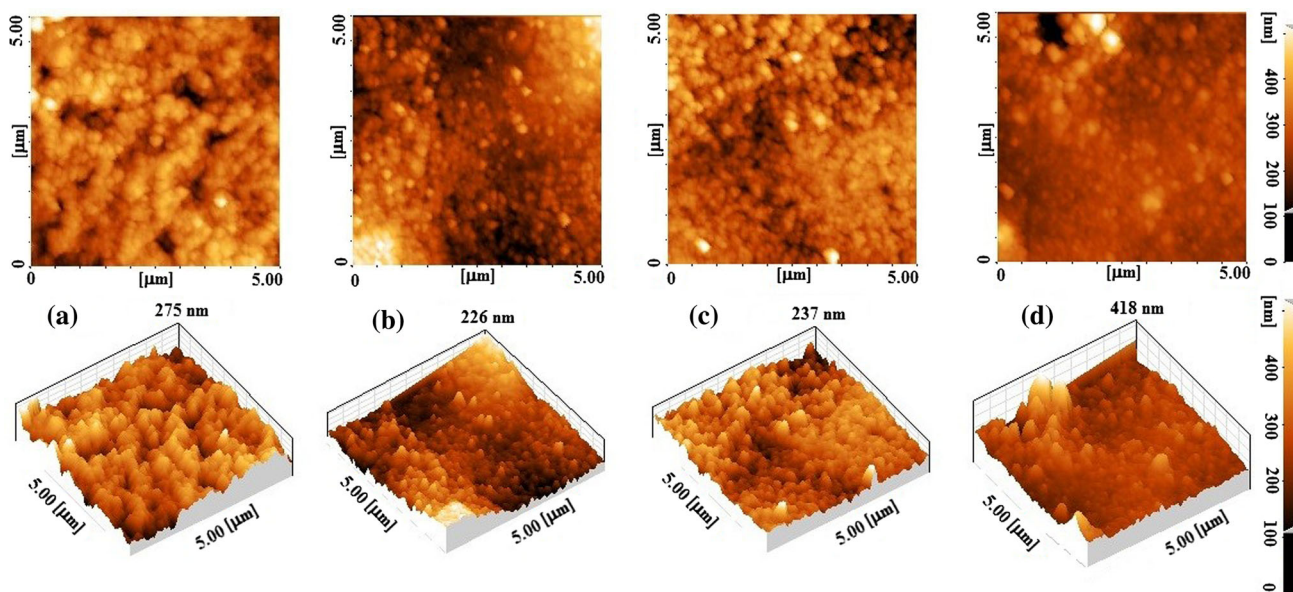
Fig. 2 AFM 2D and 3D micrographs of sprayed Cu$_2$ZnSnS$_4$ thin films prepared at **a** 260 °C, **b** 285 °C, **c** 310 °C and **d** 335 °C

Table 2 Elemental amounts used for the synthesis and EDS data of the obtained products

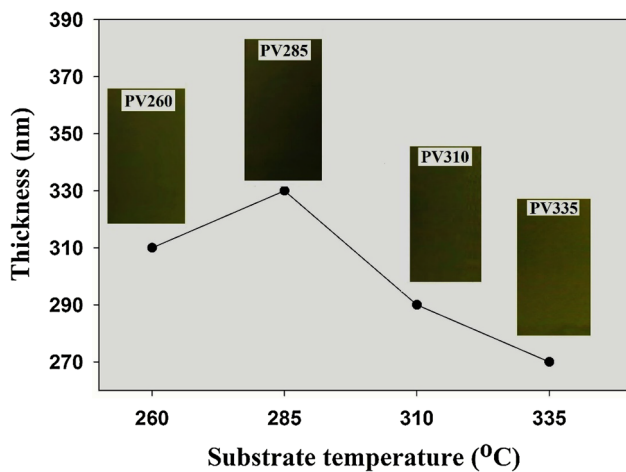| Reference	Expected molar ratios in the precursor Cu/(Zn + Sn)	Composition of elements in thin films (at%)				Cu/(Zn + Sn)	S/metal
		Cu	Zn	Sn	S		
PV260	1.00	23.43	12.34	13.53	50.70	0.90	1.03
PV285	1.00	24.14	12.66	13.09	50.11	0.93	1.01
PV310	1.00	25.94	13.14	12.77	48.15	1.01	0.93
PV335	1.00	26.19	13.01	12.14	48.66	1.04	0.94

Fig. 3 Variation of film thickness against the substrate temperature for PV samples (*Inset* figure shows photographs of PV samples at different substrate temperature of 260, 285, 310 and 335 °C with different thicknesses)

Fig. 4 Optical transmittance spectra of CZTS films

to other samples could be related to increasing of oscillations due to multiple reflections with increasing thickness [17].

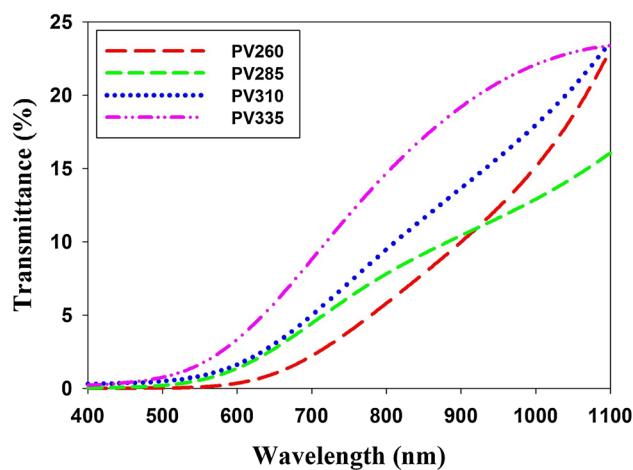In addition to transmittance spectra, the reflectance of the thin layers can also reveal some other physical properties of the samples, Fig. 5. According to these data, reflectance of the samples has a very low spectral dependence with the exception of PV285 sample. In the visible

region, where absorption is high according to the transmission diagram, reflectance of PV285 sample increases as well. This can only be explained by a theoretical treatment of the interaction between light and matter. While at the same time, a decrease in reflectance is found throughout the near-infrared (NIR) region for PV285 sample. For low energies, we observe thin-film interference effects that result from the overlaying of light that is reflected on both sides of the thin film. For PV285 sample, this effect is more visible because the thickness of this sample was greater than other samples to allow coherent overlapping of the two reflected beams.

Figure 6 shows the optical absorption coefficients, $\alpha(\lambda)$, which is estimated using the data presented in Figs. 4 and 5, i.e., the transmittance measurements, $T(\lambda)$ and the reflectance measurements, $R(\lambda)$:
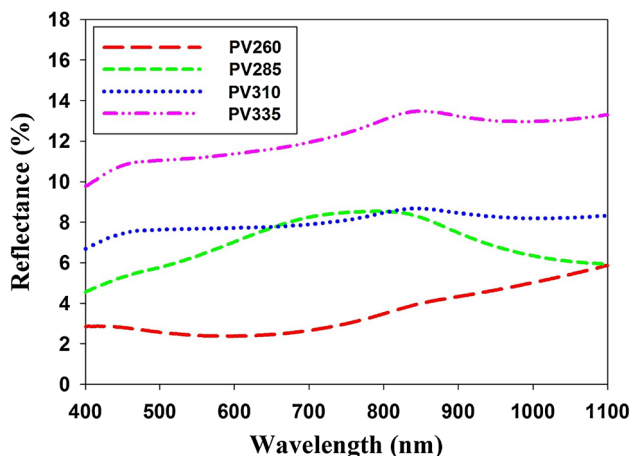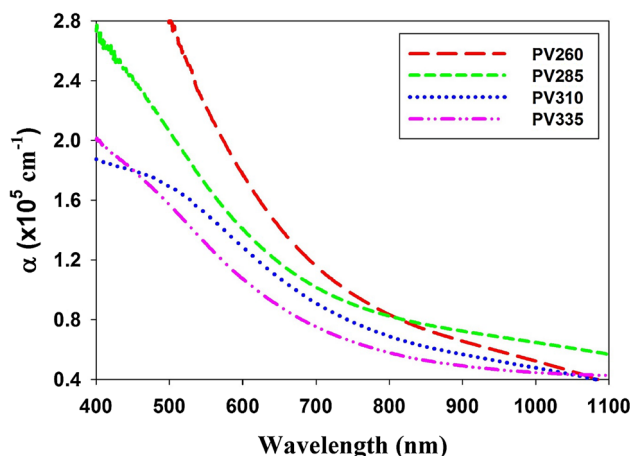
$$\alpha = \frac{1}{d}\ln\left(\frac{(1-R)^2}{T}\right) \tag{2}$$

where d is the thickness of the layers (Fig. 3). It was found that the samples presented high absorption coefficient values of about 10^5 cm^{-1}. According to these results in all samples, there is a nearly sharp absorption variation around $\lambda \approx 800$ nm. This behavior is in agreement with the band gap calculations given by the plot of $(\alpha h\nu)^{1/n}$ versus photon energy, $h\nu$, for interband transitions [18]:

$$(\alpha h\nu)^{1/n} = A\left(h\nu - E_g\right) \tag{3}$$

where A is a constant, α is absorption coefficient and the exponent n depends on the type of transition, $n = 1/2$ and 2 for direct and indirect transitions, respectively. To find the optical band gap of the samples, we have studied the variation of $(\alpha h\nu)^2$ versus photon energy, $h\nu$, Fig. 7. The presence of a straight line in the high-energy photon range confirms that the involved optical transitions occur directly across the band gap of the material. The band gap could be determined by extrapolating the straight portion to the energy axis, i.e., $(\alpha h\nu)^2 = 0$. The direct optical band gap values are found to be 1.56, 1.52, 1.48 and 1.44 eV for corresponding PV260, PV285, PV310 and PV335. As it is evident, the band gap of the films decreases as the substrate temperature increases. This reduction (red shift) could be due to the quantum confinement effect exerted by the nanosized CZTS crystals on the surface of the layers (Sects. 3.1, 3.2). The band gap of the films is quite close to the optimum band gap required for a solar cell, indicating that CZTS thin films are promising materials for solar cell application.

3.6 Electrical study

The effect of substrate temperature on the electrical properties of the CZTS films was evaluated by the Hall effect and resistivity measurements in the Van der Pauw configuration [19]. We found all the studied samples are exhibited p-type conductivity, matching well with other published reports [8–15]. The room temperature variations of Hall mobility (μ), carrier density (p) and resistivity (ρ) against the substrate temperature are shown in Fig. 8. It is evident that the trend of the hole mobility variations is consistent with the crystallite size variations (Table 1) which is in harmony with the report of Rodriguez-Lazcano et al. [20]. Also it is clear that, while the substrate temperature of the samples increases, (1) the degenerate hole density gradually increases from $\sim 2.76 \times 10^{18}$ cm^{-3} to about 4.19×10^{18} cm^{-3}; and (2) the resistivity decreases from 0.064 to 0.032 Ω cm in PV260-PV335.

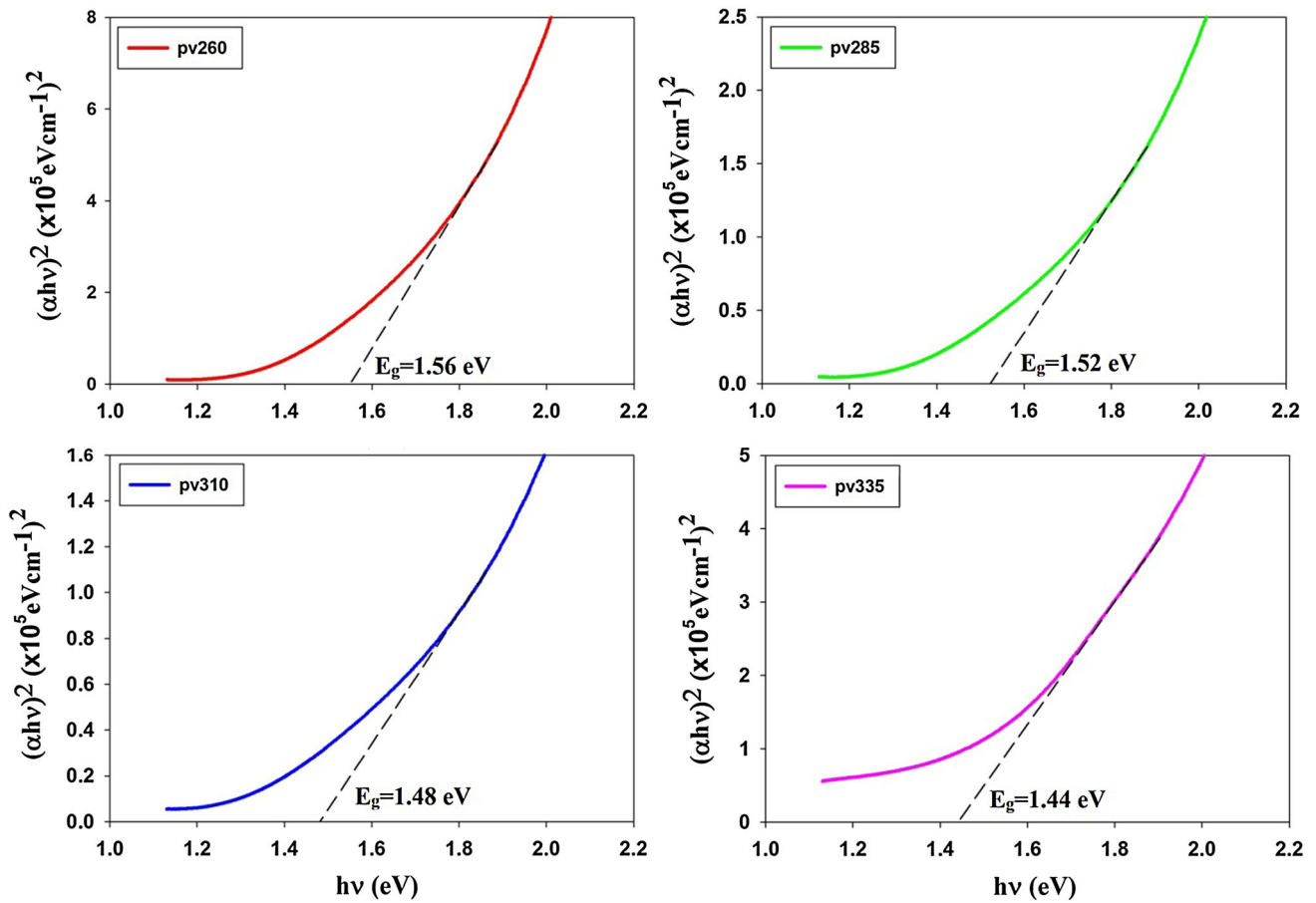The obtained values of Hall measurement are similar to the values reported for the device quality CZTS thin films

Fig. 5 Optical reflectance spectra of CZTS films

Fig. 6 Variations of absorption coefficient versus wavelength in various samples

Fig. 7 Plots of $(\alpha h\nu)^2$ versus $h\nu$ for deposited CZTS films
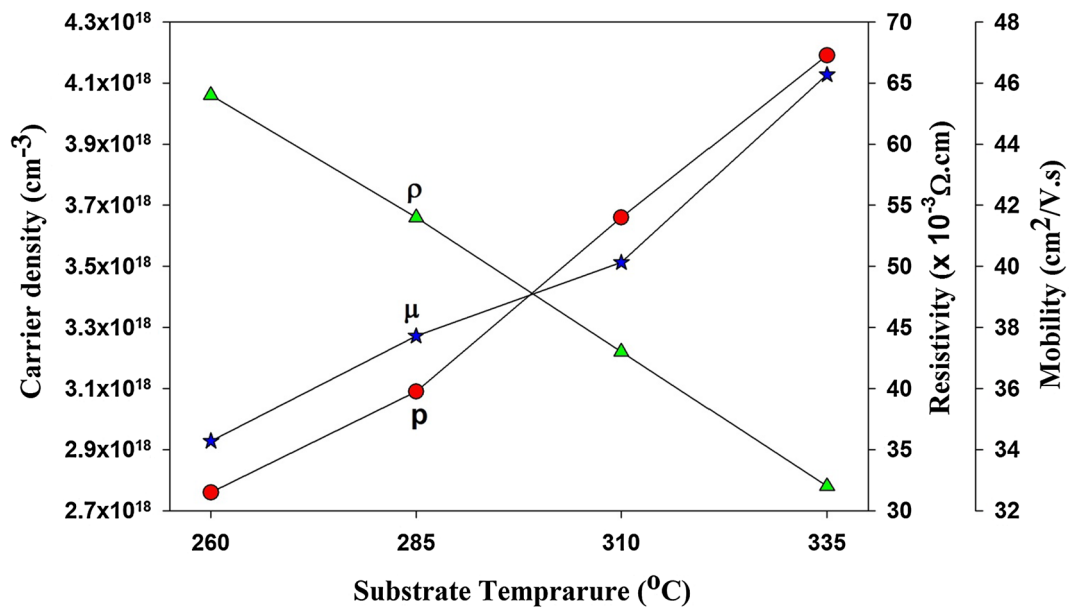

Fig. 8 Variations of resistivity (ρ), hole mobility (μ) and hole density (p) in the studied samples

[21]. Therefore, this material can be considered for single-junction solar cells.

4 Conclusions

Kesterite CZTS thin films have been grown by a spray pyrolysis technique with different substrate temperatures (260, 285, 310 and 335 °C) without sulfurization under a non-vacuum condition. We found that as substrate temperature increases: (1) the intensity of preferred (112) orientation increases, and the improvement observes in the crystallinity of spray-deposited CZTS thin films having a kesterite structure. (2) The AFM images show that a smooth, compact and crack-free morphology with reduction in the average values of roughness from 35.6 to 21.4 nm. (3) The analysis of EDX indicated that the ratio of S/metal in CZTS films is greatly affected by substrate temperature. (4) All thin films had a high absorption coefficient values close to 10^5 cm^{-1} in the visible region and the direct optical band gap in the layers decreases from 1.56 to 1.44 eV, which proves them as promising candidate for the fabrication of high-efficiency solar cells. (5) All the studied samples have degenerate p-type conductivity with a carrier density of about 10^{18} cm^{-3} which increases with the increase in the substrate temperature.

References

1. H. Matsushita, T. Maeda, A. Katsui, T. Takizawa, J. Cryst. Growth **208**, 416 (2000)
2. T. Tanaka, T. Nagatomo, T. Kawasaki, M. Nishio, Q. Guo, A. Wakahara, J. Phys. Chem. Solids **66**, 1978 (2005)
3. K. Jimbo, R. Kimura, T. Kamimura, S. Yamada, W.S. Maw, H. Araki, Thin Solid Films **515**, 5997 (2007)
4. K. Ito, T. Nakazawa, Jpn. J. Appl. Phys. **27**, 2094 (1988)
5. H. Katagiri, N. Sasaguchi, S. Hando, S. Hoshino, J. Ohashi, T. Yokota, Sol. Energy Mater. Sol. Cells **49**, 407 (1997)
6. H. Katagiri, Thin Solid Films **480–481**, 426 (2005)
7. H. Katagiri, K. Jimbo, S. Yamada, T. Kamiura, W.S. Maw, T. Fukano, T. Motohiro, Appl. Phys. Expr. **1**, 041201 (2008)
8. H. Katagiri, K. Jimbo, W.S. Maw, K. Oishi, M. Yamazaki, H. Araki, A. Takeuchi, Thin Solid Films **517**, 2455 (2009)
9. N. Nakayama, K. Ito, App. Surf. Sci. **92**, 171 (1996)
10. Y.B. Kishore Kumar, G. Suresh Babu, P. Uday Bhaskar, V. Sundara Raja, Sol. Energy Mater. Sol. Cells **93**, 1230 (2009)
11. Y.B. Kishore Kumar, G. Suresh Babu, P. Uday Bhaskar, V. Sundara Raja, Phys. Status Solidi A **207**, 149 (2010)
12. T. Kameyama, T. Osaki, K. Okazaki, T. Shibayama, A. Kudo, S. Kuwabatade, T. Torimoto, J. Mater. Chem. **20**, 5319 (2010)
13. M. Espindola-Rodriguez, M. Placidi, O. Vigil-GaÍan, V. Izquierdo-Roca, X. Fontané, A. Fairbrother, D. Sylla, E. Saucedo, A. Ṕerez-Rodŕiguez, Thin Solid Films **535**, 67 (2013)
14. N.M. Shinde, R.J. Deokate, C.D. Lokhande, J. Anal. Appl. Pyrolysis **100**, 12 (2013)
15. K. Tanaka, M. Kato, H. Uchiki, J. Alloys Compd. **616**, 492 (2014)
16. M. Adelifard, H. Eshghi, M.M. Bagheri, Mohagheghi. App. Surf. Sci. **258**, 5733 (2012)
17. S. Couve, L. Gouskov, L. Szepessy, Thin Solid Films **15**, 223 (1973)
18. J. Tauc, in *Amorphous and Liquid Semiconductors*, ed. by J. Tauc (Plenum Press, New York, 1974)
19. L.J. van der Pauw, Philips Res. Rep. **13**, 1–9 (1958)
20. Y. Rodriguez-Lazcano, H. Martinez, M. Calixto-Rodriguez, A. Nunez, Rodriguez. Thin Solid Films **517**, 5951 (2009)
21. E.M. Mkawi, K. Ibrahim, M.K.M. Ali, A.S. Mohamed, Int. J. Electrochem. Sci. **8**, 359 (2013)